model calculation[29] with a residual two-body interaction between the protons in the $f_{7/2}$ shell and the odd neutron is also successful in reproducing the features of the spectra of the three nuclei. A preliminary calculation using the shell-model wavefunction has given a value for the magnetic moment of Cr^{53} which is in better agreement with experiment than that obtained from the present calculations. A detailed comparison between the two models as applied to these nuclei should throw light on the limitations of the two models.

[29] J. R. Maxwell (private communication).

ACKNOWLEDGMENTS

The author is greatly indebted to Professor W. C. Parkinson for giving him the opportunity to work in the cyclotron laboratory and for constant encouragement; to Professor K. T. Hecht for initiating him into the theoretical analysis and for constant advice at every stage of the calculation. He is thankful to Professor B. J. Raz for helpful correspondence and to R. Leacock for help in programming. It is a pleasure to thank J. Koenig for assistance in running the experiment and Frances Hilberer for careful scanning of the nuclear emulsion plates.

PHYSICAL REVIEW VOLUME 132, NUMBER 5 1 DECEMBER 1963

Optical Model in the Interior of the Nucleus. II*

K. A. Amos† AND I. E. McCarthy†

Department of Mathematical Physics, University of Adelaide, Adelaide, South Australia, and Department of Physics, University of California, Davis, California

(Received 26 June 1963; revised manuscript received 9 August 1963)

Factors which influence the relative contribution of the interior and the surface of the nucleus to matrix elements for direct interactions involving nucleons in the entrance and exit channels are studied quantitatively. Purely optical-model effects causing localization of the reaction are phase averaging, which tends to de-emphasize the interior at all energies, and focusing which emphasizes the interior at low energies and the surface at higher energies. It is shown that phase averaging does not make the central contribution negligible at any energy. The foci in the optical-model wave functions have large effects on angular distributions. Density dependence of the two-body force for reactions which proceed by a two-body collision mechanism can be identified from angular distributions and from the energy dependence of backward cross sections which are particularly sensitive to the foci.

1. INTRODUCTION

IN a previous publication[1] (referred to as I) the question was discussed whether it is possible to infer anything about the radial localization of a direct interaction involving nucleons in the initial and final states from the general shape of the angular distributions.

The surface interaction model[2] for the excitation of collective states has had considerable success in predicting experimental results. The validity of the model is discussed particularly by Buck.[2] Direct interactions which proceed by a two-body collision in the nucleus have often been regarded also as surface effects for two main reasons.

The first concerns the optical-model wave functions which are used to represent initial and final states in the distorted-wave Born approximation (DWBA). Simple considerations[3] seem to indicate that the product particle would be likely to be reflected back into the nucleus if it came from the interior region. It was shown in I how a reduction of the interior contribution to the matrix element could arise from the fact that the phase of each partial wave of low-angular momentum is a smoother function of r in a distorted wave than in a plane wave. This effect has been called[4] "phase averaging." It is discussed for α particles by Rost.[4]

The second possible reason for reduction of the interior contribution to the matrix element is that it might be due to the reaction mechanism. For example, the fact that the Pauli principle is expected to inhibit two-body reactions more in dense nuclear matter than in the surface leads to a surface localization. There is evidence from doublet splitting that effective two-body forces in the shell model are density dependent.[5]

It was shown in I that, for low-energy direct interactions, a qualitative difference is to be expected between angular distribution shapes for surface and

* Supported in part by the Australian Institute for Nuclear Science and Engineering and the Australian Atomic Energy Commission.

† Present address: University of California, Davis, California.

[1] I. E. McCarthy, Phys. Rev. **128**, 1237 (1962).

[2] G. R. Satchler in *Proceedings of the International Symposium on Direct Interactions and Nuclear Reaction Mechanisms, Padua 1962* (Gordon and Breach Publishers, Inc., New York, 1963); B. Buck, Phys. Rev. **130**, 712 (1963).

[3] L. R. B. Elton and L. C. Gomes, Phys. Rev. **105**, 1027 (1957).

[4] N. Austern, Ann. Phys. (N. Y.) **15**, 299 (1961); E. Rost, Phys. Rev. **128**, 2708 (1962).

[5] D. C. Peaslee, Phys. Rev. **124**, 839 (1961).

volume reactions, where the reaction mechanism is assumed to be the factor causing localization to the surface region. Localization due to the optical-model wave functions was discussed and two possible effects identified, phase averaging and focusing.

The present work reports detailed calculations of angular distributions in the distorted-wave Born approximation for several representative reactions. The object is to describe more quantitatively the effects identified in I. The main conclusions are that focusing is very important in determining general characteristics of angular distributions, in particular, it can cause large backward peaks; phase averaging while it exists, is not so important; the difference between surface and volume reactions is qualitatively significant.

In Sec. 2, phase averaging is discussed and examined quantitatively in a particular case.

In Sec. 3, four reactions which might be expected to proceed by the two-body collision mechanism are studied. Angular distributions for volume interaction are compared with those for surface interaction defined by completely eliminating the contribution to the matrix element from radii less than $r_0A^{\frac{1}{3}}$, the radius parameter in the Eckart form factor used for the optical-model potential. Large differences in shape and magnitude are found. In some cases, the dependence of the differences on the parameters is discussed so that some idea can be obtained about whether the effects would be expected to be genuine features of the reaction. The effects of different assumptions about surface localization are studied.

In Sec. 4, the backward peaks which are due to focusing in the optical-model wave functions are examined for different energies, different potentials, and different radial-localization factors.

The present calculations are done with a δ-function two-body interaction, since we are interested only in the effects of the optical-model wave functions in general. For realistic fits to experimental data it is probably necessary to have a finite range force with a realistic exchange mixture, but this defect is not expected to invalidate the type of conclusions we draw here.

2. PHASE AVERAGING AND FOCUSING IN DISTORTED WAVES

The differential cross section in the distorted-wave Born approximation for incident and outgoing particles of equal mass is given by

$$d\sigma/d\Omega=\frac{k}{k'}\left(\frac{\mu}{2\pi\hbar^2}\right)^2\frac{1}{2j+1}\sum_m|\sum_{LM}\mathfrak{M}_{mML}|^2, \quad (1)$$

where k and k' are the initial and final particle momenta, μ is the reduced mass of the incident particle, j,m are the angular-momentum quantum numbers of the initial bound state (assuming that only one particle can take part in the reaction) L,M are the angular-momentum transfer and its magnetic quantum number.

$$\mathfrak{M}_{mML}=\sum_{ll'}i^{l-l'}I_{mML,ll'}Y_{l'}{}^{M}(\theta,0), \quad (2)$$

where θ is the scattering angle, l,l' are the angular momenta of the partial waves for the entrance and exit channel optical-model wave functions. Suppressing the quantum numbers m, M, L, the partial matrix elements $I_{ll'}$ are overlap integrals of the form

$$I_{ll'}=\int dr\, r^2 f_l(kr)f_{l'}(k'r)R_{npj}(r)R_{n'p'j'}(r)v(r), \quad (3)$$

where f_l and $f_{l'}$ are radial-wave functions for the entrance and exit channel optical models, R_{npj} and $R_{n'p'j'}$ are radial-wave functions for the initial and final bound states whose principal and angular-momentum quantum numbers are respectively n,p and n',p'. Harmonic-oscillator wave functions of the form given by Glendenning[6] are used in this work. The δ-function approximation to the two-body potential has been used, but its strength $v(r)$ is assumed to have a radial dependence.

It was shown in I how, in accordance with the suggestion of Austern,[4] the phases of f_l and $f_{l'}$ fall off with r more smoothly for distorted waves than for undistorted waves, thus resulting in a partial cancellation for small ($\ll kR$ where R is the nuclear radius) values of l because of phase averaging in the region where $R_{np}R_{n'p'}$ is appreciable.

Figure 1 illustrates the phases of f_l for different values of l in the case of 30-MeV neutrons on C^{12} with optical-model parameters $V=40$ MeV, $W=18$ MeV, $r_0=1.2$ F, $a=0.5$ F. It is clear that for $l<4$, which is approximately the surface value, the phase falls off quite smoothly with r, whereas for larger l, the phase curves have almost square corners as they do for plane waves, since the optical potential has little effect on these partial waves.

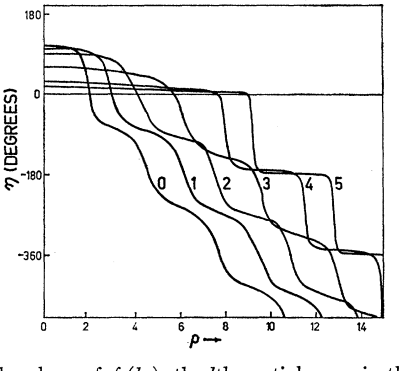

FIG. 1. The phase of $f_l(kr)$, the lth partial wave in the optical-model wave function for the scattering of 30-MeV neutrons from C^{12}, with parameters $V=40$ MeV, $W=8$ MeV, $r=1.2$ F, $a=0.5$ F. The phase is plotted against $\rho=kr$. The curves are labeled by the corresponding value of l.

[6] N. K. Glendenning, Phys. Rev. **114**, 1297 (1959).

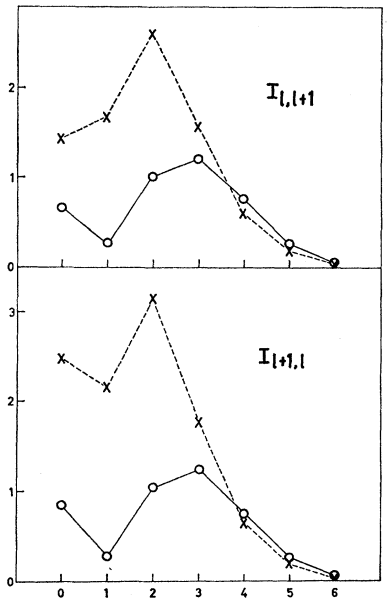

FIG. 2. The overlap integrals $I_{\frac{1}{2}01,ll'}$ and $I_{\frac{1}{2}01,l'l}$ defined in Eq. (3) plotted against l. The permissible values of l' are $l+1$ and $l-1$. The reaction is the inelastic scattering of 60-MeV protons from F^{19} for $L=1$. The circles indicate the values for the distorting potential $V=40$ MeV, $W=8$ MeV, $r_0=1.2$ F, $a=0.5$ F. The crosses indicate the values for distortion by the Coulomb potential but no nuclear potential.

Phase averaging gives a reduction in magnitude of $I_{ll'}$ for small l. It is not a particularly large reduction in the case of nucleons in the entrance and exit channels as can be seen from Fig. 2, where $I_{\frac{1}{2}01,ll'}$ and $I_{\frac{1}{2}01,l'l}$ are plotted against l for the inelastic scattering of 60-MeV protons on F^{19} causing excitation from the $\frac{1}{2}+$ ground state to the $\frac{1}{2}-$ first excited state. The values for fully distorted waves are compared with the values for waves distorted by the Coulomb potential only. $v(r)$ is taken to be constant.

Distortion also produces a phase change in the $I_{ll'}$. It was shown in I how the phase relationships of the partial waves produce focusing in the wave function. For fairly low energies (<30 MeV), as can be seen in Fig. 1, there are differences of up to 90° in the phases of successive partial waves for $l \cong kR$ (excluding the 90° difference arising from the factor i^l) which are capable of roughly reversing the direction of some of the $I_{ll'}$ relative to others so that at a scattering angle of 180°, where the cross section is small in the plane-wave theory due to cancellations among the $I_{ll'}$, it is possible to get reinforcement for distorted waves giving backward peaks. Backward peaks do not appear at high energies when the phase differences between successive partial waves are not large enough to cause significant constructive interference at 180°.

Phase averaging, resulting in a reduction of the magnitude of $I_{ll'}$ for small l,l', is expected to show up in dwBa angular distributions as a reduced dependence of the angular distribution on the center of the nucleus. Focusing, connected with the phases of the $I_{ll'}$ which are very different for successive l,l' in the surface region, large but not very different for successive small l,l' and small for large l,l', is expected to show up in DWBA angular distributions as backward peaking. The backward peaks are dependent on the energy and angular momentum transfer.

3. THE CONTRIBUTION TO THE DWBA FROM THE NUCLEAR INTERIOR

In order to see the effect of completely removing the contribution from the nuclear interior ($r<r_0A^{\frac{1}{3}}$) in different reactions at incident energies of 5 and 10 MeV, angular distributions were calculated using the potentials given in Table I. The potentials were the same in both exit and entrance channels.

The angular distributions for 5 MeV and 10 MeV are plotted in Figs. 3(a) and 3(b). The plots are on a linear scale to emphasize the peaks. The vertical scale is changed arbitrarily from curve to curve in order to facilitate comparison of shapes. In each case, the values of the differential cross section for surface interaction have been multiplied by a factor of about 100. This means that the contribution of the interior to the matrix elements is about 10 times that of the surface with this definition of the surface.

At 5 MeV, although the shapes of the angular distributions for volume and surface interaction are different, the differences are perhaps not so great that they could not be removed by reasonable changes of parameters.

At 10 MeV, systematic differences become obvious. The surface cases show more structure. They are compressed towards small angles as would be expected from the larger average radius, so that where backward peaks occur for volume interaction, they are shifted towards smaller angles for surface interaction and the backward cross section is relatively small. This effect is observed in all the cases except $Ca^{40}(n,p)K^{40}$ which is too complicated to generalize about.

It is interesting to compare odd L cases with even L cases. For this purpose, we will discuss $F^{19}(p,p')F^{19*}$ and $C^{13}(p,n)N^{13}$. Because of the parity rule,[7] the F^{19} case

TABLE I. Potentials used in volume and surface reaction calculations.

Reaction	E (MeV)	V (MeV)	W (MeV)	r_0 (F)	a (F)	L
$F^{19}(p,p')F^{19*}$	5	45	4	1.2	0.55	1
	10	55	4	1.2	0.55	
$C^{13}(p,n)N^{13}$	5	55	4	1.2	0.55	0
	10	55	4	1.2	0.55	
$In^{115}(p,p')In^{115*}$	5	45	4	1.2	0.55	5
	10	45	4	1.2	0.55	
$Ca^{40}(n,p)K^{40}$	5	45	4	1.2	0.55	3, 5
	10	45	4	1.2	0.55	

[7] A. J. Kromminga and I. E. McCarthy, Phys. Rev. Letters **6**, 62 (1961).

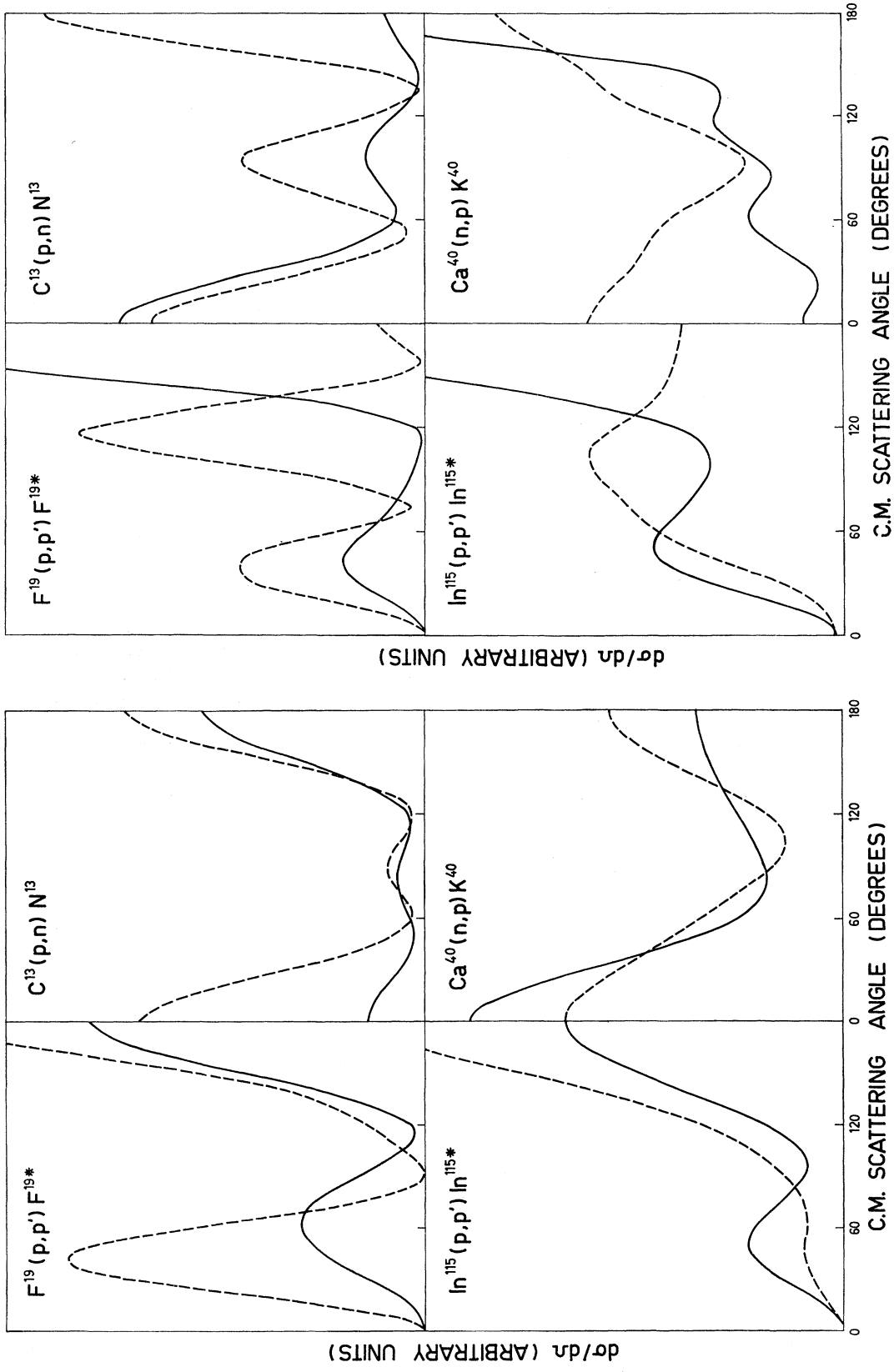

FIG. 3. (a) The angular distributions for 5 MeV and (b) 10 MeV incident energy for the reactions listed in Table I. The continuous line indicates volume interaction, the broken line indicates surface interaction. The vertical scale factors have no significance from one curve to another. The vertical scale is linear.

is constrained to have very small forward cross section. The backward peak is the major qualitative feature that will be discussed.

Figure 4 shows that, for the F^{19} case at 10 MeV, changing the real part of the optical-model potential from 45 to 55 MeV has little effect on the backward peak for volume interaction but decreases it by a factor of 3 for surface interactions without much changing the general shape of the curve. In terms of the focus overlap explanation of backward peaks,[8] this means that the focus is brought a little nearer to the center of the nucleus by the increase in potential and that this has a small relative effect when the whole focus plays a part, but a larger relative effect when we omit the contribution to the matrix element from all but the edge of the focus. This behavior of the foci is illustrated in Fig. 5.

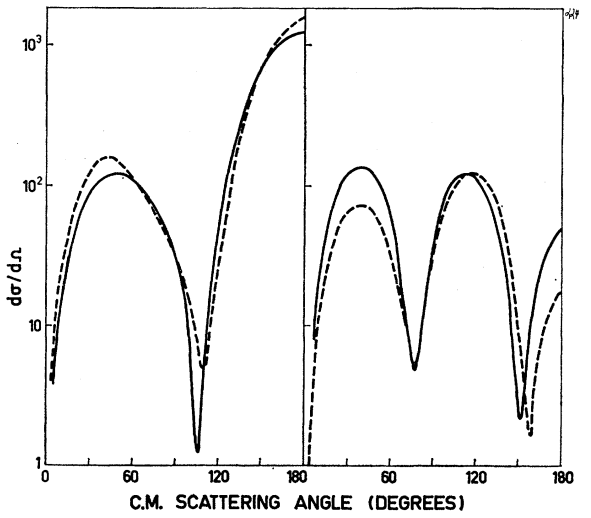

FIG. 4. Angular distributions for the reaction $F^{19}(p,p')F^{19*}$ with $L=1$ at 10 MeV. Volume interaction is on the left, surface interaction on the right. The continuous lines indicate calculations done with $V=45$ MeV. The broken lines are for $V=55$ MeV. Other parameters are those of Table I. The curves on the right have been multiplied by 100. The units on the vertical scale are arbitrary, but consistent from curve to curve.

The other parameters are found to have less effect than V on the shape. Increasing W decreases the magnitude of the cross section by roughly a constant factor. These curves are plotted logarithmically. The scale factors for each volume interaction curve are equal. The scale factors for each surface interaction curve are equal and 100 times those for volume interaction.

Figure 6 shows the C^{13} case at 10 MeV. The surface interaction scale factor is 1000 times the volume interaction scale factor. In this case, where L is even, both forward and backward peaks are strongly dependent on the foci. For volume interaction, increasing the potential from 45 to 55 MeV has a large effect on the backward peak, but not on the forward peak, without qualitatively

[8] I. E. McCarthy and D. L. Pursey, Phys. Rev. 122, 578 (1961).

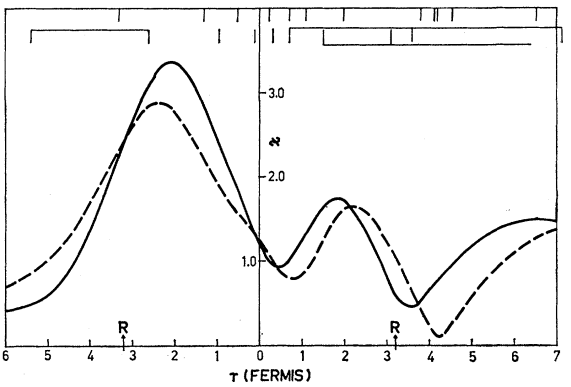

FIG. 5. The magnitude χ and phase of the optical-model wave function for the entrance channel in the cases shown in Fig. 4 calculated on the scattering axis. The broken line is for $V=45$ MeV, the continuous line is for $V=55$ MeV. The top row of marks at the top of the diagram indicates the phase for the broken line. The marks are at intervals of 50°. The bottom row is for the continuous line. Marks representing equal phases are linked.

changing the shape of the angular distribution. For surface interaction, the increase in the potential causes more of the focus to miss the interaction region with a resulting general decrease in cross section. The focal behavior in each channel is shown in Fig. 7.

The greatly reduced magnitude for surface reaction matrix elements is of course due to the fact that only the tail of the bound-state wave function contributes. It is necessary to examine different definitions of surface interaction to see how the cross sections depend on them.

This has been done for the $L=1$ $F^{19}(p,p')F^{19*}$ case. First, the shape of the angular distribution must depend strongly on the reduction factor between central and

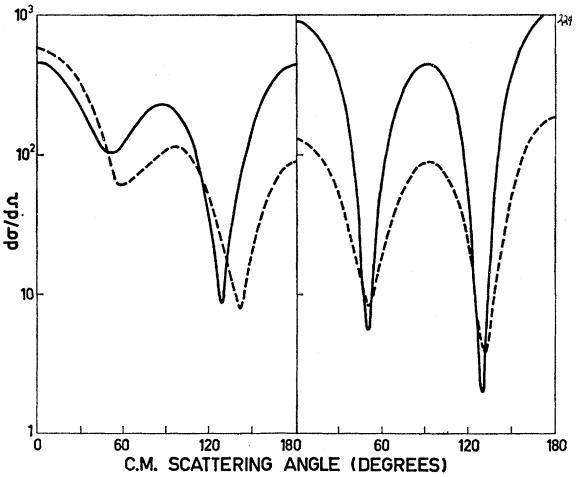

FIG. 6. Angular distributions for the reaction $C^{13}(p,n)N^{13}$ with $L=0$ at 10 MeV. Volume interaction is on the left, surface interaction on the right. The continuous lines are for $V=45$ MeV, the broken lines are for $V=55$ MeV. Other parameters are those of Table I. The curves on the right have been multiplied by 1000. The units on the vertical scale are arbitrary, but consistent from curve to curve.

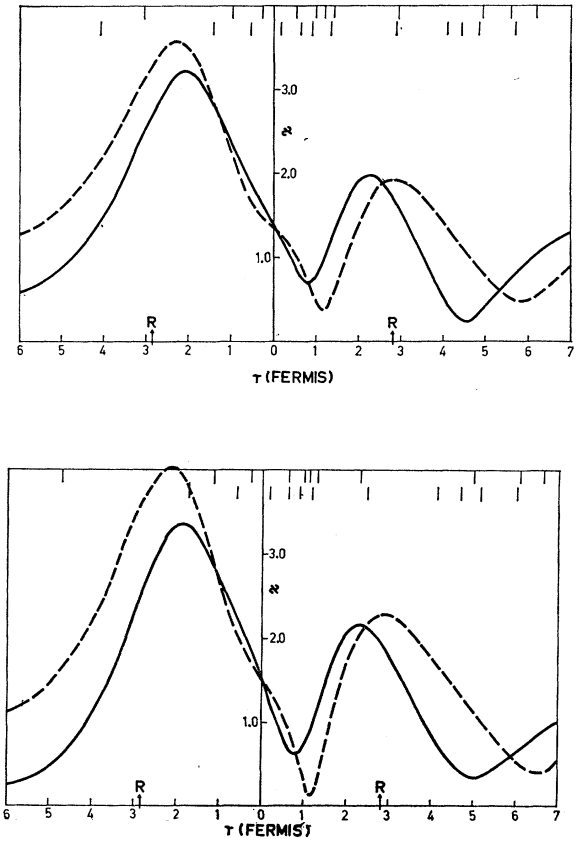

FIG. 7. Magnitudes χ and phases (indicated by marks as for Fig. 5) of the entrance (top) and exit (bottom) channel optical-model wave functions for the cases of Fig. 6. The broken line is for $V=45$ MeV, the continuous line is for $V=55$ MeV.

surface interaction. It is unlikely that reactions would be purely confined to the surface. Calculations have been done with a square-form factor giving the radial dependence of the interaction potential $v(r)$.

$$v(r)=f, \quad r\leqq R_f.$$
$$v(r)=1, \quad r>R_f.$$

The incident energy used was 10 MeV and the parameters were those of Table I. The radius R of the Eckart form factor is about 3.2 F in this case.

For $R_f=R$, $f=0.5$, it was found that the shape of the angular distribution was indistinguishable from that in the case $f=1$ (volume interaction), but the magnitude was reduced by a factor 4. Clearly, this calculation corresponds merely to a volume calculation with a reduced potential $v(r)$ and a slightly different tail. The intermediate cases will have similar shapes to the extreme cases unless the central and surface parts of the overlap integrals are of the same order of magnitude.

When R_f was reduced to 2.2 F, with $f=0$, it was found that the three peaks characteristic of surface interaction remained, but the backward peak was much higher than the first peak, indicating that the interaction region now included a significant amount of the foci.

Figure 8 shows two intermediate cases where the magnitudes of the cross sections are roughly similar. In one case we have larger R_f and larger f than the other. The values used were $R_f=2.2$ F and 1.8 F and $f=0.5$ and 0 respectively. The third peak characteristic of surface interaction is still present in each curve but the backward peaks are large in each case. The magnitudes of the backward peaks are 0.7 of the value for $f=1$.

The angular distribution was also calculated using a form factor $v(r)$ which was the derivative of the Eckart form factor. Three peaks were again observed.

It is fairly clear that in this reaction a tendency to surface weighting is shown by the appearance of a peak at about 90°, which seems to be quite a critical test of the surface weighting assumption. It would perhaps be surprising if refinements to the calculation such as inclusion of spin-orbit coupling in the optical model and a more realistic two-body force would change this qualitative conclusion. Further work is planned on this point. The experiment would be well worth doing.

Surface and volume interaction has also been compared in the F^{19} case at energies up to 60 MeV. It is a

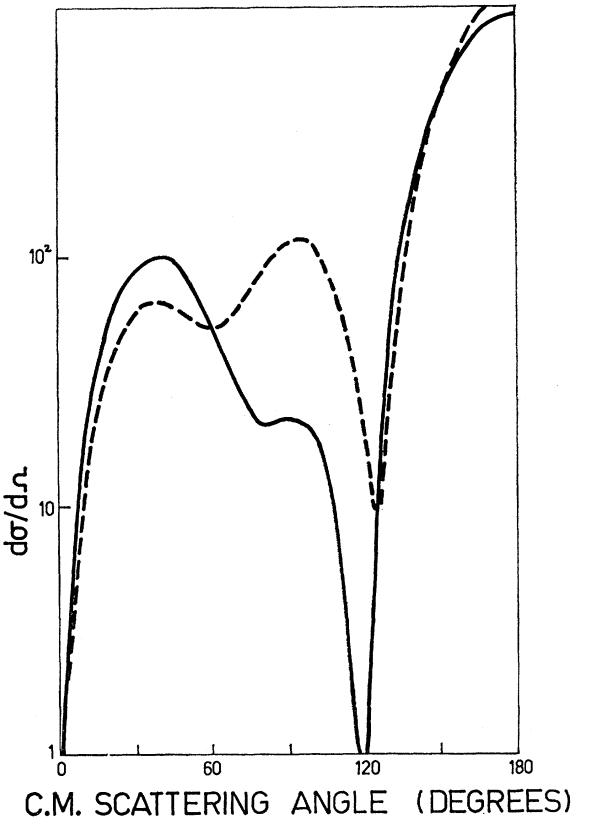

FIG. 8. Angular distributions for the inelastic scattering of 10-MeV protons from F^{19} with $L=1$. The parameters are those of Table I. The continuous line represents the calculation with $R_f=2.2$ F, $f=0.5$, the broken line is for $R_f=1.8$ F, $f=0$.

general rule that there are more peaks in the surface interaction angular distributions than the volume interaction ones. Focusing certainly is not a property of the interior at higher energies, so there is no doubt that the interior contribution to the matrix element is important in determining the angular distribution, independent of focusing. Hence, there is no purely optical-model effect such as phase averaging or total internal reflection that makes the interior contribution unimportant.

The qualitative conclusions that can be drawn from these examples are as follows.

In general, there are significant differences between angular distributions for volume and purely surface interactions. In the case of $L=1$ reactions on light nuclei, the difference is extremely marked, with three peaks in the 10 MeV surface interaction case and only two in the 10 MeV volume interaction case. The general fact that surface interactions have more peaks than volume interactions persists at energies up to at least 60 MeV.

The differences are most marked near 180° in all cases, while they are also important at 0° for parity-preserving reactions. The nature of the differences depends on the real part of the potential, the qualitative dependence being understandable on the picture of focus overlap causing backward peaks. The energy dependence of the backward peaks is different for different potentials as well as for different localization assumptions. In the next section the backward peaks will be examined in more detail in particular cases.

Surface-reaction matrix elements, which include only the tail of the bound-state wave function, are considerably smaller in magnitude than those for volume interaction. The magnitude depends strongly on the exact manner in which the surface interaction is defined.

Intermediate cases between volume and pure surface interaction generally show characteristics of both so that there is hope of identifying them experimentally.

4. FOCUS EFFECTS IN DWBA ANGULAR DISTRIBUTIONS

It has previously been shown[8] how backward peaks can arise in the distorted-wave Born approximation from the fact that, at 180° the foci in the entrance and exit channels overlap. At backward angles the other large parts of the optical-model wave functions, namely the surface parts on the same side of the nucleus as the incident or outgoing particle in the entrance and exit channels, respectively, also overlap, so that two fairly distinct regions of space contribute to the matrix element. Interference between these "surface" and "focus" contributions results in variation of the height of the backward peaks with energy.[9] At forward angles the focus of one wave function overlaps the surface part of the other. The focus is mainly responsible for the forward peaks in parity-preserving reactions with $L>0$. Because of the rather sharp division of the parts of space contributing to the backward matrix element, the backward peaks should depend rather critically on the optical-model properties of the matrix element, which we are considering here, and less on the details of the two-body interaction. The position of the foci, in particular, should be very important.

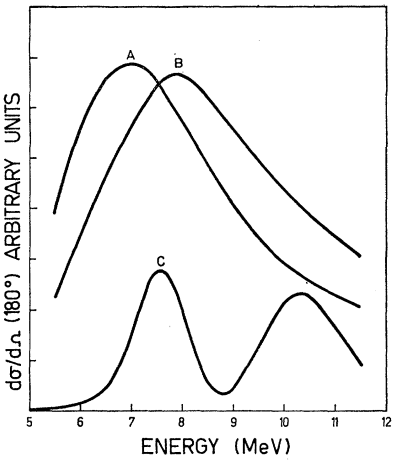

FIG. 9. The differential cross section at 180° for $C^{13}(p,n)N^{13}$ as a function of energy. Curves (A) and (B) are for $V=50$ and 47 MeV, respectively, and $W=6$ MeV, $r_0=1.2$ F, $a=0.55$ F, $R_b=2.3$ F, $f=1$. Curve (C) is for $V=50$ MeV, $W=6$ MeV, $r_0=1.2$ F, $a=0.55$ F, $R_b=2.2$ F, $R_f=2.2$ F, $f=\frac{1}{16}$.

Energy variation of the backward cross section may also be due to the positions of the foci. These are determined by the incident energy and the real parts of the optical-model potentials. Variation of the imaginary parts of the optical-model potentials with energy produces variation of the focal intensities and, hence, variation of the backward cross section.

For low energies and large V, the focus is near the center of the nucleus. As the energy increases or V decreases it moves out to larger radii. Radial variation of the bound-state wave functions therefore produces energy variation of the focal contribution to the matrix element. A semiclassical model of this effect has been calculated by Pearson.[10]

The variation of the backward cross section with energy and potential has been studied for the reaction $C^{13}(p,n)N^{13}$ for which experimental data are available[11] at incident energies between about 3.5 and 13 MeV. The experimental distribution with energy of the backward cross section shows a strong peak at about 6 MeV and possibly a second peak between 8 and 9 MeV. The points are widely scattered due, no doubt, to effects of more or less isolated resonances, but the general trend would be expected to be given by direct interaction theory.

Figure 9 shows the energy variation of the backward

[9] A. J. Kromminga and I. E. McCarthy, Nucl. Phys. **24**, 36 (1961).

[10] C. A. Pearson (to be published).

[11] P. Dagley, W. Haeberli, and J. X. Saladin, Nucl. Phys. **24**, 353 (1961).

cross section using the following parameters in both entrance and exit channels. $V=50$ MeV, for curves (A) and (C), 47 MeV for curve (B), $W=6$ MeV, $r_0=1.2$ F, $a=0.55$ F. The radius R_b of the $1p$ bound-state wave function used in each channel was 2.3 F for curves (A) and (B), 2.2 F for curve (C). This is unrealistically small. Two different shapes for the radial two-body form factor $v(r)$ were used, namely $f=1$ (volume interaction) for curves A and B, and $f=1/16$, $R_f=2.2$ F. This value of f gives center and surface contributions to the matrix element of the same order of magnitude. Only the shapes of the curves are significant.

The most striking fact about the curves of Fig. 9 is that the energy variation of the backward cross section reflects the shape of the factor

$$R_{npj}(r)R_{n'p'j'}(r)v(r)$$

in the overlap integral for the matrix element. In this case, the same $1p$ harmonic-oscillator wave function was used for both entrance and exit channels. The radial factor has one peak in the $f=1$ case. A peak might be expected to appear in the energy distribution when the focus is situated at the radius of the peak in the wave functions. The peak is at a higher energy for curve (B) than for curve (A). This is contrary to the simple picture because the focus should be at a slightly larger radius for smaller V. However, the situation is complicated by focus-surface interference. The relative phase of the surface and focus contributions changes rapidly with V and energy and the same situation would be expected to arise at lower energy for higher V. The large Q value of -3.005 MeV means also that the entrance and exit channel foci occur at different radii. The magnitude and phase of the entrance channel wave function at 5 and 10 MeV are shown in Fig. 10.

Curve (C) shows that, when the surface is weighted more than the center, the backward cross section increases again as the foci enter the heavily weighted region.

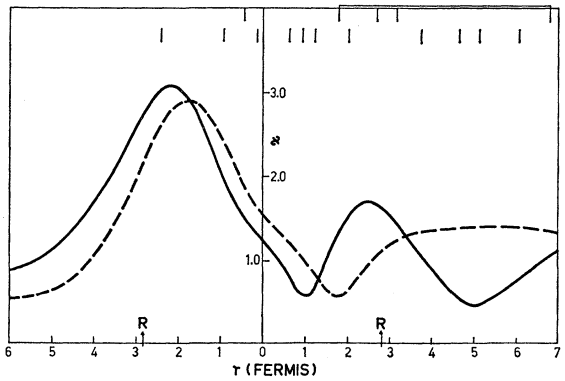

FIG. 10. Magnitudes χ and phases (indicated by marks as for Fig. 5) of the entrance-channel wave functions at 5 MeV (broken line) and 10 MeV (continuous line) on the scattering axis for case A of Fig. 9.

The variation of the optical-model potentials with energy is also a complicating factor. However, this variation should at least be monotonic, so any significant tendency to a second peak in the energy variation curve could indicate surface weighting. It was found that, in this energy region, the increase in W with energy was the most important determining factor in the shape of the energy distribution, causing it to drop quickly at higher energies.

The effect of the foci in producing forward peaks in cases where L is even and greater than zero is illustrated in Fig. 11 for the inelastic scattering of protons from the second excited state of F^{19}. Here $L=2$. The parameters were those of Table I. The curves on the left are for 10 MeV, those on the right for 20 MeV incident energy. The shapes only are significant. The solid curves are for $f=1$, the dashed curves for $f=0$, $R_f=R$.

In the 10 MeV case for surface interaction, the focus is in the central region, so the forward cross section is small. At 20 MeV, the focus is in the surface region. The relative heights of forward and backward peaks are the same in this case for surface and volume interactions. This may, however, be just an accident at the particular energy.

5. CONCLUSIONS AND DISCUSSIONS OF EXPERIMENTS

Purely optical-model effects such as phase averaging do not significantly reduce the contribution of the interior of the nucleus to the distorted-wave Born approximation matrix elements at any energy. Significant differences between surface and volume interaction mechanisms persist at high energy and show up in angular distributions.

At energies up to about 30 MeV the shapes of angular distributions are greatly affected by the foci in the optical-model wave functions. The movement of the focus from small to large radii as the energy increases

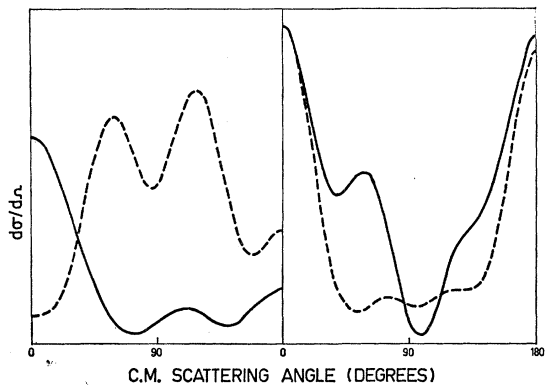

FIG. 11. Angular distribution for the inelastic scattering of 10 MeV (left side) and 20 MeV (right side) protons from the second excited state of F^{19} with $L=2$. Continuous lines are for volume interaction, broken lines are for surface interaction. The parameters are $V=55$ MeV, $W=4$ MeV, $r_0=1.2$ F, $A=0.55$ F, $R_b=R_f=3.2$ F.

should give a sensitive test of the assumption that the surface is more heavily weighted than the center due to the reaction mechanism. The energy dependence of focus effects such as backward peaks should show up any substantial surface weighting.

These general conclusions could be tested by observing the energy dependence of backward cross sections for known collective excitations where the surface weighting assumption is reasonably well established.

It has been shown in Sec. 3 that the magnitude of the cross section is very sensitive to the surface weighting factor. Although the zero-range potential assumption is too crude to expect fits to angular distributions, it is useful to compare the magnitudes of the cross sections with the experimental ones[11] in the case of $C^{13}(p,n)N^{13}$ with different assumptions about surface weighting.

The two-body potential will be written as

$$U(|\mathbf{r}_1-\mathbf{r}_2|)=4\pi\mu^{-3}U_0v(r_1)\delta(|\mathbf{r}_1-\mathbf{r}_2|)$$

in order to compare it with the Yukawa potential (μ is the range parameter set equal to 1.15 F^{-1}). For $f=1$ we find $U_0\approx 60$ MeV, whereas in the extreme case $f=0$, $R_f=R$, a value of $U_0\approx 1000$ MeV must be used. Intermediate cases have intermediate values according to the rough proportionality rules illustrated in Sec. 3. 60 MeV is roughly comparable with the value of U_0 for free nucleon-nucleon scattering.

In this context it is interesting to note that a calculation[12] performed by Agodi and Schiffrer with a realistic potential including finite range and exchange for the reaction $Si^{28}(n,p)Al^{28}$ at 14 MeV required values of U_0 larger by a factor of between two and three than the one determined from the free n-p interaction. Hence, it is clear that there appears to be an effect of nuclear matter on the two-body scattering operator of a large enough magnitude to be observed according to the considerations of Sec. 3 (see particularly the discussion of Fig. 8, where an effect of density dependence on the angular distribution is noticeable when there is a ratio of only 0.7 between the magnitudes of the curves for the surface weighting and volume interaction cases compared with the ratio of 0.1 to 0.5 between U_0^2 for free particles and the value of U_0^2 for the effective potential in $Si^{28}(n,p)Al^{28}$).

A program of future work is planned in which the considerations of the present work will be investigated with an improved model including surface absorption, finite range forces with exchange, and spin-orbit coupling. It is not hoped to fit angular distributions until this is done. The effect of exchange forces in particular on the forward cross section for $Si^{28}(n,p)Al^{28}$ is to improve experimental agreement significantly.[12]

[12] A. Agodi and G. Schiffrer, Nucl. Phys. (to be published); A. Agodi, R. Giordano, and G. Schiffrer, Phys. Letters 4, 253 (1963).

ACKNOWLEDGMENTS

We would like to thank Dr. C. A. Pearson for useful discussions, Dr. J. R. Rook, Dr. P. E. Hodgson, and Dr. B. A. Robson for helping us check our distorted wave code, Dr. A. Agodi and Dr. G. Schiffrer for prepublication information, and the staff of the Adelaide University Computing Center and Weapons Research Establishment, S. A. Salisbury, for cooperation with computing problems.